X-ray Crystal Structure of Thorium Tetrahydroborate, $Th(BH_4)_4$, and Computational Studies of $An(BH_4)_4$ (An = Th, U)

Andrew C. Dunbar,[a] Joseph C. Wright,[a] Daniel J. Grant,[b] and Gregory S. Girolami*,[a]

[a] School of Chemical Sciences, University of Illinois at Urbana-Champaign. 600 South Mathews Ave., Urbana, IL 61801, U.S.A.

[b] Department of Chemistry, University of Minnesota and Supercomputing Institute, 207 Pleasant St. SE, Minneapolis, MN 55455, U.S.A.

■ **ABSTRACT:** The crystal structure of $Th(BH_4)_4$ is described. Two of the four BH_4^- ions are terminal and tridentate (κ^3) whereas the other two bridge between neighboring Th^{IV} centers in a κ^2,κ^2 (i.e., bis-bidentate) fashion. Thus, each thorium center is bound to six BH_4^- groups by 14 Th–H bonds. The six boron atoms describe a distorted octahedron in which the κ^3-BH_4^- ions are mutually *cis*; the 14 ligating hydrogen atoms define a highly distorted bicapped hexagonal antiprism. The thorium centers are linked into a polymer consisting of interconnected helical chains wound about four-fold screw axes. The structures of $An(BH_4)_4$ (An = Th, U) were also investigated by DFT. The geometries of $[An(BH_4)_6]^{2-}$, $[An_3(BH_4)_{16}]^{4-}$, and $[An_5(BH_4)_{26}]^{6-}$ fragments of the polymeric structures were optimized at the B3LYP and/or PBE levels. Most calculated geometries are 14-coordinate and agree with the experimental structures, but isolated $[Th(BH_4)_6]^{2-}$ units are predicted to feature 16-coordinate Th^{IV} centers.

■ INTRODUCTION

Metal tetrahydroborates are fascinating compounds with several real and potential applications, including organic synthesis, hydrogen storage, electroless plating, and the synthesis of nanomaterials.[1-7] One of the first such compounds discovered was $U(BH_4)_4$, which was evaluated during World War II as the transporting agent in the separation of fissile ^{235}U from uranium ores by gas diffusion.[8-9] Interest in $U(BH_4)_4$ for this purpose stemmed from the fact that it was one of the few volatile uranium compounds known. Ultimately, $U(BH_4)_4$ was rejected in favor of UF_6 because the hexafluoride can withstand higher temperatures without decomposing (and thus can generate higher vapor pressures of uranium-bearing material). Today the relatively high volatilities of metal tetrahydroborates make them useful as precursors for the chemical vapor deposition of metal diboride phases;[10-20] the latter materials are hard, high-melting, wear- and corrosion-resistant, and electrically conductive.[21-26]

Uranium(IV) tetrahydroborate, also known as uranium(IV) borohydride, is a polymer in the solid state. Single-crystal X-ray and neutron diffraction studies carried out in 1972 revealed that each uranium center in $U(BH_4)_4$ is surrounded by six tetrahydro-borate groups, four of which bridge adjacent metal centers in a κ^2,κ^2 fashion.[27-28] The two remaining BH_4^- ligands are terminal on uranium, bound in a κ^3 fashion, and mutually *cis*. Thus each uranium center is bonded to 14 hydrogen atoms in all, endowing $U(BH_4)_4$ with the highest coordination number then known for any molecular complex. The 14 hydrogen atoms describe a distorted bicapped hexagonal antiprism as the coordination polyhedron.

Interestingly, in 1979 a new polymorph of $U(BH_4)_4$ was discovered that is orthorhombic instead of tetragonal.[29] In this orthorhombic phase, each uranium center is also bound to four bridging κ^2-BH_4^- ligands and two terminal κ^3-BH_4^- ligands, but the latter are mutually *trans* rather than *cis*.[30] As a result, the bridging BH_4^- ions form a 2D polymeric network that is quite

different from the 3D network seen in the tetragonal polymorph. The U···B distances for the κ^2- and κ^3-BH_4^- ligands are similar in the two forms, however.

Shortly after $U(BH_4)_4$ was first described,[8] the thorium analogue was prepared.[31] Powder X-ray diffraction investigations by Zachariasen suggested that $Th(BH_4)_4$ and the tetragonal form of $U(BH_4)_4$ are isomorphous;.[31] this conclusion was subsequently confirmed by Banks.[32] The IR spectra of $Th(BH_4)_4$ and $U(BH_4)_4$ also support this conclusion: B–H stretching bands are seen at 2555 (m), 2545 (s), 2505 (m), 2440 (m), 2285 (s), 2235 (s), 2200 (s), and 2118 (s) cm^{-1} for $Th(BH_4)_4$ and at 2552 (m), 2538 (s), 2262 (s), 2182 (s), and 2087 (s) cm^{-1} for $U(BH_4)_4$.[33] The strong bands at high frequency (2450-2600 cm^{-1}) and the strong doublets at low frequency (2100-2200 cm^{-1} with a splitting of 50-80 cm^{-1}) are diagnostic[9, 34] of tridentate BH_4^- ligands.[34-36] Bands typically observed for bidentate BH_4^- ligands (strong doublets in the range 2400-2600 cm^{-1}) are evidently obscured by those due to the tridentate groups, but the presence of bidentate BH_4^- is suggested by the peaks of medium intensity at 2555 (Th) and 2552 (U) cm^{-1} and by the strong peaks at 2118 (Th) and 2087 (U) cm^{-1}. Interestingly, $M(BH_4)_4$ complexes of neptunium and plutonium are monomeric (as are the related compounds of the transition elements Zr and Hf) owing to the smaller sizes of these metals.[32, 37-39]

Despite powder diffraction and spectroscopic data indicating that $Th(BH_4)_4$ and the tetragonal form of $U(BH_4)_4$ are isomorphous, their physical and chemical properties are rather different. For example, whereas $Th(BH_4)_4$ sublimes only with difficulty at 130 ºC (P_{vap} = 0.05 Torr at this temperature)[31] and is thermally stable up to its melting point of 204 ºC, the uranium analogue sublimes readily at 30 ºC (P_{vap} = 0.19 Torr)[31] and decomposes at 100 ºC.[8] In addition, the thorium compound is far less soluble in nonpolar, non-coordinating solvents than its uranium analogue.

Although $Th(BH_4)_4$ was first prepared more than 70 years ago, the details of its solid-state structure have remained unknown. Here we report the single-crystal structure of $Th(BH_4)_4$ and DFT studies of both it and the uranium analogue.

■ RESULTS AND DISCUSSION

Synthesis and Crystal Structure of $Th(BH_4)_4$. Two preparations of thorium tetrahydroborate have been reported. The original 1949 synthesis by Hoekstra and Katz entailed treatment of ThF_4 with the pyrophoric reagent $Al(BH_4)_3$ in the absence of a solvent.[31] Twenty years later, Ehemann and Nöth reported that $Th(BH_4)_4$ could be isolated by treatment of $ThCl_4$ with $LiBH_4$ in diethyl ether followed by removal of the solvent and sublimation in vacuum.[40] We find that the product obtained by the latter route tends to retain substoichiometric amounts of diethyl ether, which complicates efforts to obtain single crystals of the desolvated material.

Accordingly, we employed the original Hoekstra and Katz method to prepare all samples of $Th(BH_4)_4$ used in the present study. Colorless crystals suitable for X-ray diffraction were grown by sublimation under vacuum at 150 °C. These $Th(BH_4)_4$ crystals conform to the space group $P4_32_12$, with four formula units per unit cell and half a molecule per asymmetric unit. Selected distances and angles are given in Table 1. As we will show, the structure is isomorphous with that of tetragonal $U(BH_4)_4$.

The thorium centers reside on special positions with two-fold rotational site symmetry (Wyckoff position *a*). All thorium centers have the same coordination geometry: two BH_4^- ions are terminal (centered on B2 and the symmetry-related atom B2A) and bond to thorium in a tridentate κ^3 mode whereas the other two anions per formula unit (centered on B1 and its symmetry-related atoms) bridge between neighboring thorium centers in a bis-bidentate or κ^2,κ^2 fashion (Figure 1). The bridging nature of the latter adds two BH_4 groups to the

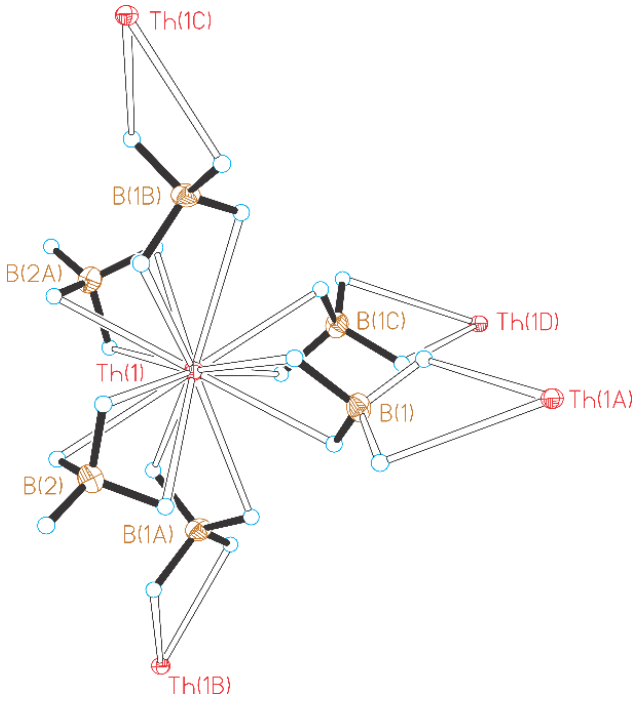

Figure 1. Molecular structure of $Th(BH_4)_4$. Ellipsoids are drawn at the 30% probability level except those for hydrogen atoms, which are represented by arbitrarily sized spheres. See Table 1 for symmetry codes.

coordination sphere of each thorium atom. Thus, each Th center is bound to six BH_4^- groups overall (two of which are terminal and four of which are bridging) by means of a total of 14 Th–H bonds (2 × 3 + 4 × 2). Coordination numbers exceeding 10 are not uncommon for Th^{IV}, but a coordination number of 14 is noteworthy; even Th_4H_{15}, the higher of the two well-characterized thorium hydrides, features metal centers that are "merely" 12-coordinate.[41] Here the 14 ligating hydrogen atoms do not define a simple coordination polyhedron, but it is possible to view their arrangement in terms of a highly distorted bicapped hexagonal antiprism.[27-28]

If one ignores the hydrogen atoms, the six boron atoms about each thorium center describe a distorted octahedral arrangement in which the two terminal κ^3-BH_4^- groups are mutually *cis*. The angle between these two ligands is 108.2(3)°; unsurprisingly, this is the largest angle

between two mutually *cis* BH_4^- groups in the structure. The crystallographic two-fold axis passes through thorium, bisecting the B···Th···B angle defined by the two κ^3-BH_4^- groups; a view down this axis is shown in Figure 2. The two-fold axis is perpendicular to the B···Th···B axis described by the bidentate BH_4^- ligands that are mutually *trans*. If we regard these two BH_4^- groups as "axial" groups, then the four "equatorial" groups are disposed alternately above and below the mean plane that they define. Undoubtedly this distortion serves to maximize the non-bonded H···H distances between different BH_4^- groups.

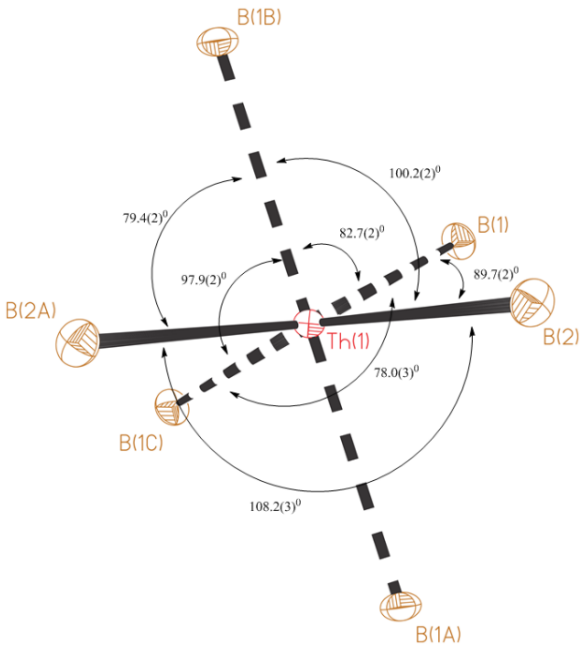

Figure 2. View down the crystallographic two-fold axis that passes through the Th^{IV} center. Ellipsoids are drawn at the 30% probability level; hydrogen atoms have been deleted for clarity. Solid lines indicate linkages to κ^3-BH_4^- groups, whereas dashed lines denote linkages to κ^2-BH_4^- groups. Angles not marked are B(1A)···Th(1)···B(1B) = 179.3(3)º and B(2)···Th(1)···B(1C) = 156.6(2)º.

The Th···B distance of 2.570(6) Å for each terminal κ^3 tetrahydroborate ion is similar to distances reported for the other known thorium complexes bearing tridentate BH_4^- ligands: 2.61(3) Å in $Th(BH_4)[N(SiMe_3)_2]_3$,[42] 2.48(2)-2.60(2) Å in $Th_2(H_3BMe)_8(OEt_2)$,[43] 2.61(8)-

2.632(9) Å in $Th_2(H_3BMe)_8(THF)$,[43] 2.49(6)-2.71(7) Å in $Th(H_3BCH_3)_4$,[44] 2.618(7) and 2.624(3) Å in the bis(permethylindenyl) complex $(C_9Me_7)_2Th(BH_4)_2$,[45] 2.640(1)-2.673(3) Å for the series of terphenolate complexes $(OTer^{Mes})_2Th(BH_4)_2(DME)$, $(OTer^{Mes})_2Th(BH_4)_2$, and $[(OTer^{Mes})_2Th(BH_4)_2(4,4'\text{-}NC_5H_4C_5H_4N)]_\infty$ [$OTer^{Mes}$ = *O*-2,6-(2,4,6-$Me_3C_6H_2$)C_6H_3],[46] and most recently 2.627(5) Å in $(C_5Me_5)_2Th(BH_4)_2$.[47]

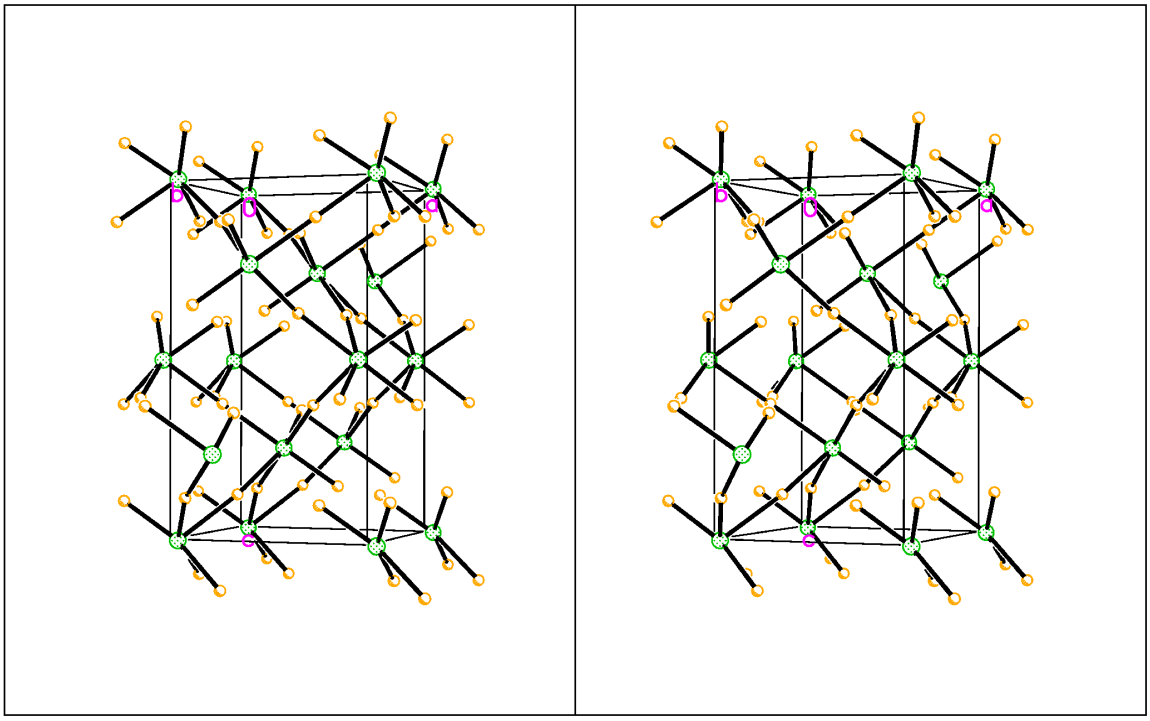

Figure 3. Stereoscopic view perpendicular to the *c*-axis with hydrogen atoms removed for clarity. Key: larger circles are Th, smaller circles are B.

Interestingly, $Th(BH_4)_4$ is only the second thorium compound shown to contain both κ^3- and κ^2-BH_4^- groups. The other such compound is the 1,2-bis(dimethylphosphino)ethane complex $Th(BH_4)_4(dmpe)_2$, in which the κ^3 Th···B distances are 2.694(8)-2.686(9) Å and the κ^2 Th···B distances are 2.879(9)-2.950(8) Å.[48] The κ^2 Th···B distances of 2.895(6) and 2.934(6) Å in $Th(BH_4)_4$ are thus similar to the corresponding values for $Th(BH_4)_4(dmpe)_2$ and also comparable to those in the 15-coordinate aminodiboranate complex $Th(H_3BNMe_2BH_3)_4$, which range from 2.882(3) to 2.949(3) Å.[49] As a final point of comparison,

[MeC(^{i}PrN)$_2$]$_3$Th(H$_2$BC$_8$H$_{14}$) exhibits a κ^2 Th···B distance of 2.952(9) Å associated with its bulky boranate ligand deriving from 9-borabicyclo[3.3.1]nonane.[50]

The powder X-ray diffraction pattern calculated from the single-crystal data (Figure S1) agrees with that reported for Th(BH$_4$)$_4$ by Banks and Edelstein.[37] Our cell parameters, a = 7.6073(4) Å and c = 13.3631(9) Å, are also consistent with those found in the earlier study [a = 7.58(3) Å and c = 13.31(5) Å].[37]

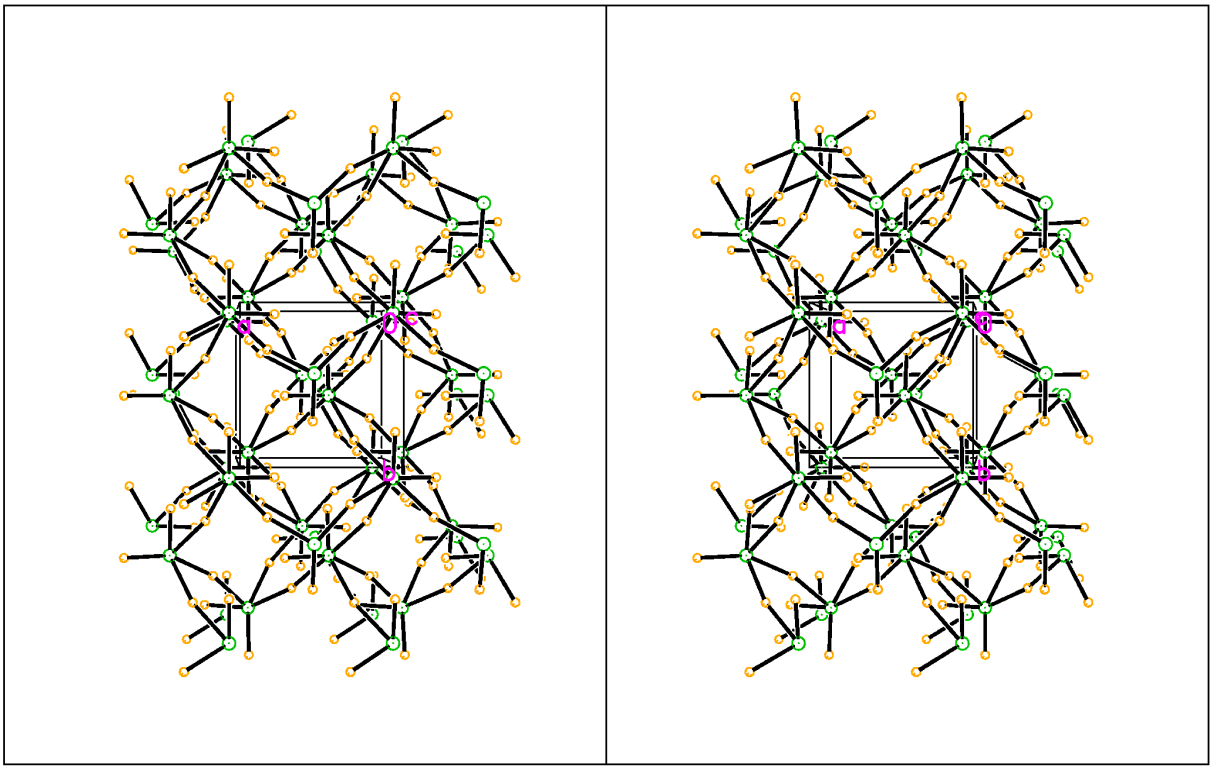

Figure 4. Stereoscopic view down the *c*-axis with hydrogen atoms removed for clarity. Key: larger circles are Th, smaller circles are B.

Comparison of the Structures of Th(BH$_4$)$_4$ and Tetragonal U(BH$_4$)$_4$. It is of interest to compare the structure of Th(BH$_4$)$_4$ with that of the isomorphous tetragonal form of U(BH$_4$)$_4$, for which both X-ray and neutron diffraction studies are available.[27-28] This form of U(BH$_4$)$_4$ also crystallizes in the $P4_32_12$ space group; the cell parameters are slightly smaller than those

for $Th(BH_4)_4$ (Table S1), as expected from the smaller size of U^{IV}. In both $Th(BH_4)_4$ and tetragonal $U(BH_4)_4$, the MB_6 octahedra are linked by vertex-sharing into three-dimensional polymers that consist of interconnected helical chains wound about four-fold screw axes that are parallel to the *c*-axis of the unit cell (Figures 3 and 4). Additional vertex sharing links the octahedra into zig-zag chains that run parallel to the *a* and *b* axes.

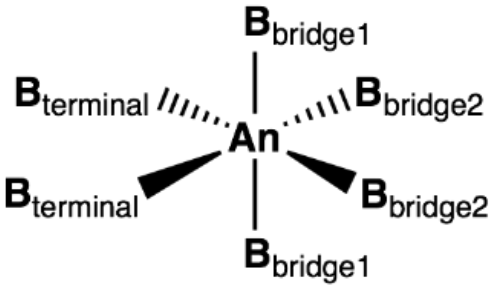

Figure 5. Labeling scheme for the six boron atoms about each metal center in tetragonal $An(BH_4)_4$ (An = Th, U).

These structures exhibit three crystallographically distinct An···B distances (Figure 5): the An···B_t distances to the terminal tridentate tetrahydroborates, the An···B_{b1} distances to the bridging bidentate tetrahydroborate ligands that are *trans* to one another, and the An···B_{b2} distances to the bridging bidentate tetrahydroborate ligands that are *trans* to the κ^3 tetrahydroborates.

The An···B_t distance in $U(BH_4)_4$, 2.52(1) Å (neutron) or 2.53(3) Å (X-ray), is 0.04-0.05 Å shorter than the analogous distance of 2.570(6) Å in $Th(BH_4)_4$—a finding that accords with the 0.06-Å difference in ionic radii of Th^{IV} and U^{IV}.[51] Similarly, the U···B_{b1} distance, 2.90(1) Å (neutron) or 2.85(3) (X-ray), is at least 0.03 Å shorter than the Th···B_{b1} distance of 2.934(6) Å. This trend continues with the An···B_{b2} distances: the value of 2.88(3) Å (X-ray) or 2.82(2) Å (neutron) for $U(BH_4)_4$ is 0.02-0.07 Å shorter than that of 2.895(6) Å in $Th(BH_4)_4$. We can conclude that the An···B distances track the radius of the actinide ion fairly closely.

One interesting feature is that, in both the U and Th structures, the An···B_{b2} distances (approximately *trans* to the κ^3 tetrahydroborates) are about 0.04-0.08 Å shorter than the An···B_{b1} distance (*trans* to one another). This difference may indicate the operation of a *trans* influence, in which the κ^3-BH_4^- ligand is a weaker *trans*-directing group than κ^2-BH_4^-. *Trans* influences[52] (and inverse *trans* influences)[53-55] in *f*-element chemistry are known. Alternatively, the difference may reflect steric effects involving the BH_4^- ligands.

Finally, we point out that the appreciably lower volatility of $Th(BH_4)_4$ relative to $U(BH_4)_4$ suggests that the bridging interactions in the former compound are stronger than those in the latter, thus creating a larger energetic barrier for depolymerization of $Th(BH_4)_4$ to monomers or small oligomers. This behavior could simply be a consequence of the larger radius of Th^{IV}—and thus a higher energetic cost associated with the decrease in coordination number upon depolymerization of the solid-state structure—but it could also reflect greater ionicity in the Th^{IV}-BH_4^- interactions.

Computational Results.[49, 56-58] DFT calculations were implemented to determine whether the details of the solid-state structures of $Th(BH_4)_4$ and $U(BH_4)_4$ can be reproduced theoretically. Because calculations on extended polymers are impractical for various reasons,

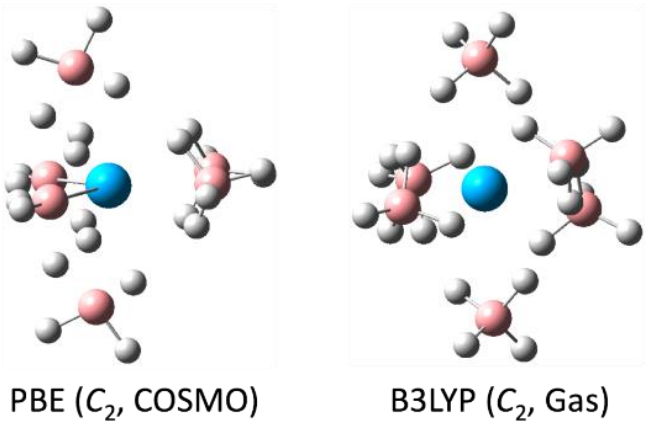

Figure 6. Optimized molecular structures for 14-coordinate $[Th(BH_4)_6]^{2-}$ at the RI-PBE/def-TZVP and B3LYP/aug-cc-pVTZ levels. Th, blue; B, pink; and H, white.

we instead optimized the structures of several fragments of the 3D polymeric structures adopted by these tetrahydroborate complexes. The fragments have formulas $[An(BH_4)_6]^{2-}$, $[An_3(BH_4)_{16}]^{4-}$, and $[An_5(BH_4)_{26}]^{6-}$. The $[An(BH_4)_6]^{2-}$ unit represents a single An center and its six surrounding BH_4^- ligands, four of which bridge to nearby An centers in the experimentally determined structure. The An_3 and An_5 clusters represent larger polymer fragments in which two and four BH_4^- ions, respectively, of a central $[An(BH_4)_6]^{2-}$ unit link to other An centers. Thus $[An_3(BH_4)_{16}]^{4-}$ has the connectivity $(BH_4)_4An[-(\mu\text{-}BH_4)\text{-}An(BH_4)_5]_2$ and the $[An_5(BH_4)_{26}]^{6-}$ fragment has the connectivity $(BH_4)_2An[-(\mu\text{-}BH_4)\text{-}An(BH_4)_5]_4$.

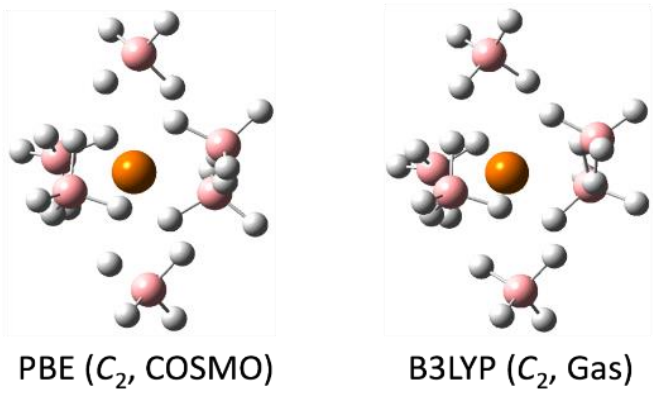

Figure 7. Optimized molecular structures for 14-coordinate $[U(BH_4)_6]^{2-}$ at the RI-PBE/def-TZVP and B3LYP/aug-cc-pVTZ levels. U, gold; B, pink; and H, white.

Selected optimized geometry parameters at the PBE and B3LYP levels for $[Th(BH_4)_6]^{2-}$ and $[U(BH_4)_6]^{2-}$ are reported in Tables 2 and 3, respectively, and selected optimized geometry parameters at the PBE level for $[An_3(BH_4)_{16}]^{4-}$ and $[An_5(BH_4)_{26}]^{6-}$ (An = Th, U) are reported in Table 4. The final optimized molecular structures at the PBE and B3LYP levels for $[Th(BH_4)_6]^{2-}$ are depicted in Figure 6 and those for $[U(BH_4)_6]^{2-}$ in Figure 7; optimized structures for $[An_3(BH_4)_{16}]^{4-}$ and $[An_5(BH_4)_{26}]^{6-}$ (An = Th, U) at the PBE level are depicted in Figures 8 and 9, respectively.

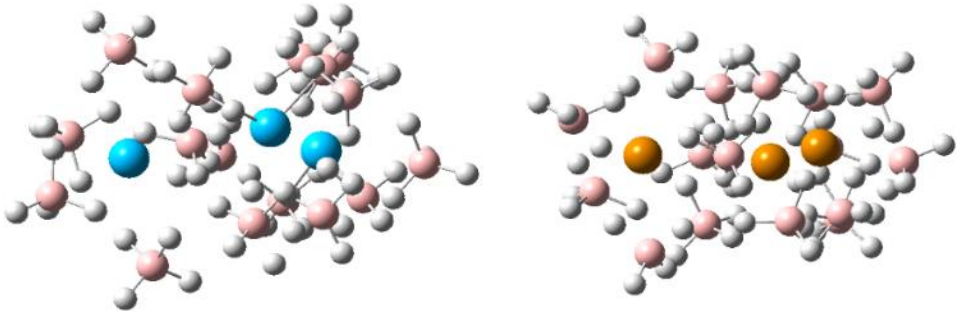

Figure 8. Optimized molecular structures for 14-coordinate $[An_3(BH_4)_{16}]^{4-}$ (An = Th, U) at the RI-PBE/def-TZVP level. Th, blue; U, gold; B, pink; and H, white.**4.**

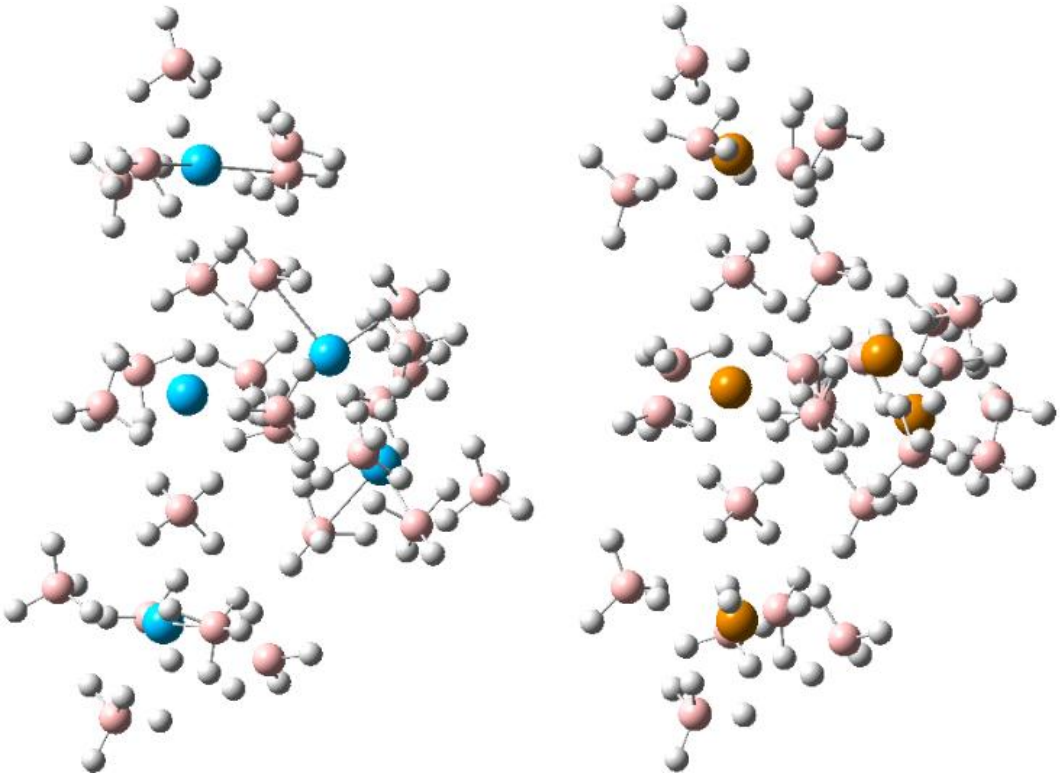

Figure 9. Optimized molecular structures for 14-coordinate $[An_5(BH_4)_{26}]^{6-}$ (An = Th, U) at the RI-PBE/def-TZVP level. Th, blue; U, gold; B, pink; and H, white.

1. $[Th(BH_4)_6]^{2-}$. Geometry optimizations were performed both in the gas phase and in solvent (COSMO) at two levels of theory, namely PBE/def-TZVP and B3LYP/aug-cc-PV*n*Z (aV*n*Z, *n* = D, T). In general, the effect of solvent is to reduce the Th···B distances by ~0.02 Å while increasing variation in the B···Th···B angles by a few degrees. Initial geometry

optimizations at the RI-PBE/def-TZVP level were performed by constraining the ions to have 14-coordinate $[Th(\kappa^3\text{-}BH_4)_2(\kappa^2\text{-}BH_4)_4]^{2-}$ structures with C_2 symmetry; this symmetry requires the two tridentate ligands to be mutually *cis*. With this symmetry, however, a vibrational frequency analysis indicated the optimized C_2 structures (both gas-phase and COSMO) to be characterized by three imaginary frequencies. Furthermore, the optimized geometry differed significantly from the experimental crystal structure.

Relaxing the initial symmetry constraints and reoptimizing the 14-coordinate structure at the RI-PBE/def-TZVP level leads to a lower-energy structure in which the two $\kappa^2\text{-}BH_4^-$ groups *trans* to the $\kappa^3\text{-}BH_4^-$ ions are now also tridentate. In essence, the structure rearranges to become 16-coordinate: two of the BH_4^- groups remain bidentate while four become tridentate. This rearranged structure is lower in energy in both the gas phase and COSMO optimizations. Vibrational frequency analyses confirmed that this 16-coordinate structure indeed corresponds to a local minimum, having no imaginary frequencies. In fact, in work we will report elsewhere, the experimental crystal structure of the $[Th(BH_4)_6]^{2-}$ ion, i.e., in which no BH_4^- group bridges to another Th center, has this 16-coordinate structure with four $\kappa^3\text{-}BH_4^-$ groups.

In order to investigate the effect of functional and basis set, geometry optimizations were performed at the PBE and B3LYP levels with the aVDZ and aVTZ basis sets. At the PBE/aVTZ level, $[Th(BH_4)_6]^{2-}$ is also predicted to be 16-coordinate; the optimized structure is very similar to the PBE/def-TZVP structure (C_1 symmetry, COSMO, Table 2). Interestingly, however, at the B3LYP/aVTZ level $[Th(BH_4)_6]^{2-}$ optimizes to a 14-coordinate structure (C_2 symmetry, gas) that is more comparable to the experimental crystal structure of $Th(BH_4)_4$. The $Th\cdots B_t$ distance to the tridentate tetrahydroborate ligands is overestimated by 0.104 Å, whereas the $Th\cdots B_{b1}$ and $Th\cdots B_{b2}$ distances to the bidentate tetrahydroborate ligands are only 0.010 and 0.026 Å too long, respectively. The $B_t\cdots Th\cdots B_t$ angle differs by a relatively large amount (15°)

compared to the experimental value. The $B_{b1}\cdots Th\cdots B_{b1}$ and $B_{b2}\cdots Th\cdots B_{b2}$ angles between the bidentate BH_4^- ions differ by 9 and 16°, respectively.

Frequency calculations were performed to determine the nature of the optimized structure. At the PBE/aVTZ level, the optimized structure is a true minimum, but at the B3LYP/aVTZ level, there are two small imaginary frequencies of 14 and 77 cm^{-1}. The hybrid B3LYP functional predicts not only the experimentally observed coordination number of 14 but also more reasonable geometry parameters compared to the PBE functional. However, agreement with experiment is still not entirely satisfactory, requiring the optimization of larger segments of the polymeric $Th(BH_4)_4$ structure (see below).

2. $[U(BH_4)_6]^{2-}$. Following a similar procedure, geometry optimizations of the uranium species $[U(BH_4)_6]^{2-}$ have been performed both in the gas phase and in solution (COSMO) at the PBE/def-TZVP level, as well as in the gas phase at the PBE and B3LYP levels with the aVDZ and aVTZ basis. Irrespective of functional and basis set, all levels predict a 14-coordinate structure. In general, geometry optimizations in solvent lead to a shortening of the U···B distances by an average of ~0.02 Å, whereas the B···U···B angles show a slightly larger variation by as much as 9°. At the RI-PBE/def-TZVP (C_1 symmetry, COSMO) level, the $U\cdots B_t$ distance is slightly longer than experiment by 0.014 Å, and the $U\cdots B_{b1}$ and $U\cdots B_{b2}$ distances are slightly underestimated by 0.056 and 0.009 Å, respectively. The predicted B3LYP/aVTZ (C_2 symmetry, gas) structure also shows good agreement with experiment; the tridentate and bidentate U···B distances are overestimated by 0.070 and 0.010-0.043 Å, respectively.

3. $[Th_3(BH_4)_{16}]^{4-}$ (3Th) and $[Th_5(BH_4)_{26}]^{6-}$ (5Th). In **3Th**, $[Th(BH_4)_5]^-$ units are appended to the two bidentate BH_4^- ligands opposite the tridentate BH_4^- ligands in $[Th(BH_4)_6]^{2-}$. In **5Th,** on the other hand, $[Th(BH_4)_5]^-$ units are appended to all four bidentate BH_4^- groups in $[Th(BH_4)_6]^{2-}$. In going from **3Th** to **5Th**, the $Th\cdots B_t$ distance remains essentially fixed at 2.67 Å whereas the $Th\cdots B_{b1}$ and $Th\cdots B_{b2}$ distances decrease by 0.034 and

0.060 Å, respectively. The Th···B_t, Th···B_{b1}, and Th···B_{b2} distances of **5Th** are calculated to be 0.104 Å longer and 0.031 and 0.043 Å shorter, respectively, compared to the experimental crystal structure. The B···Th···B angles of **3Th** and **5Th** are calculated to be within a couple degrees of each other. In general, the B···Th···B angles of **5Th** are in reasonable agreement with the experimental values except for the angles between the tridentate BH_4^- groups and the bidentate BH_4^- groups, which show the largest discrepancies of 9 and 12°, respectively.

4. $[U_3(BH_4)_{16}]^{4-}$ (3U) and $[U_5(BH_4)_{26}]^{6-}$ (5U). The connectivities in $[U_3(BH_4)_{16}]^{4-}$, **3U**, and $[U_5(BH_4)_{26}]^{6-}$, **5U**, are the same as in their thorium analogues. In going from **3U** to **5U**, the U···B distances marginally decrease by 0.013 Å. Similarly, the B-U-B angles of **5U** are all within 3° of the analogous angles in **3U**. In a comparison of the geometry parameters of **5U** with those of the experimental crystal structure, the U···B_t, U···B_{b1}, and U···B_{b2} distances are underestimated by 0.019, 0.078, and 0.011 Å, respectively. In general, the B···U···B angles of **5U** are in reasonable agreement with the experimental values. The B_t···U···B_t angle is calculated to be 9° smaller whereas the computed B_{b1}···Th···B_{b1} and B_{b2}···Th···B_{b2} angles are 9° smaller and 8° larger, respectively.

■ CONCLUSIONS

We have determined the crystal structure of $Th(BH_4)_4$ and confirmed that this compound is isomorphous with the tetragonal form of its uranium analogue. The thorium centers are linked into a three-dimensional polymer consisting of interconnected helical chains wound about four-fold screw axes. Our computational studies show that the geometries for $[An(BH_4)_6]^{2-}$ fragments of the polymeric structures differ for the two actinides: the optimized geometry is 16-coordinate when An = Th but 14-coordinate when An = U. The 14-coordinate structure is stable for thorium only when two or four of the BH_4^- ligands in $[An(BH_4)_6]^{2-}$ bridge

to other Th^{IV} centers. Inclusion of these bridging interactions renders the theoretical calculations fully consistent with the crystallographic results.

■ ASSOCIATED CONTENT

The Supporting Information is available free of charge at xxxxx.

Preparative details, single-crystal structure analysis, and computed powder diffraction pattern for $Th(BH_4)_4$, and details of computational methods (PDF)

Accession Codes

CCDC 2078975 contains the supplementary crystallographic data for this paper. These data can be obtained free of charge via www.ccdc.cam.ac.uk/data_request/cif, or by emailing data_request@ccdc.cam.ac.uk, or by contacting The Cambridge Crystallographic Data Centre, 12 Union Road, Cambridge CB2 1EZ, UK; fax: +44 1223 336033.

■ AUTHOR INFORMATION

Corresponding Author

Gregory S. Girolami – School of Chemical Sciences, University of Illinois at Urbana-Champaign. 600 South Mathews Ave., Urbana, IL 61801, U.S.A. ORCID: 0000-0002-7295-1775

E-mail: ggirolam@illinois.edu

Authors

Andrew C. Dunbar and Joseph C. Wright – School of Chemical Sciences, University of Illinois at Urbana-Champaign. 600 South Mathews Ave., Urbana, IL 61801, U.S.A.

Daniel J. Grant – Department of Chemistry, University of Minnesota and Supercomputing Institute, 207 Pleasant St. SE, Minneapolis, MN 55455, U.S.A.

Notes

The authors declare no competing financial interest.

■ ACKNOWLEDGMENTS

G.S.G. acknowledges funding from the National Science Foundation (CHE-19-54745), which supported the work of A.C.D. and the U.S. Department of Energy (DOE), Office of Science, Office of Basic Energy Sciences, Separation Science Program, under Award DE-SC0019021, which supported the work of J.C.W. We thank Dr. Danielle Gray and Amy Fuller of the George L. Clark X-Ray Facility at the University of Illinois at Urbana-Champaign for collecting the X-ray diffraction data. We also thank Prof. Laura Gagliardi, formerly of the University of Minnesota and now at the University of Chicago, for her valuable advice and assistance.

■ REFERENCES

Table 1. Selected bond lengths and angles for $Th(BH_4)_4$ at 193 K.[a]

Bond Lengths (Å)

Th(1)···B(1)	2.895(6)	Th(1)–H(3)	2.38(4)	B(1)–H(1)	1.17(5)
Th(1)···B(1A)	2.934(6)	Th(1)–H(4)	2.45(3)	B(1)–H(2)	1.15(4)
Th(1)···B(1B)	2.934(6)	Th(1)–H(5)	2.37(3)	B(1)–H(3)	1.16(4)
Th(1)···B(1C)	2.895(6)	Th(1)–H(6)	2.42(3)	B(1)–H(4)	1.19(5)
Th(1)···B(2)	2.570(6)	Th(1)–H(7)	2.41(3)	B(2)–H(5)	1.13(4)
Th(1)···B(2A)	2.570(6)			B(2)–H(6)	1.21(4)
				B(2)–H(7)	1.09(4)
				B(2)–H(8)	1.09(4)

Bond Angles (°)

B(1)···Th(1)···B(1A)	97.9(2)	B(1A)···Th(1)···B(1B)	179.3(3)
B(1)···Th(1)···B(1B)	82.66(3)	B(1A)···Th(1)···B(2)	79.4(2)
B(1)···Th(1)···B(1C)	78.0(3)	B(1A)···Th(1)···B(2A)	100.2(2)
B(1)···Th(1)···B(2)	89.7(2)	B(2)···Th(1)···B(2A)	108.2(3)
B(1)···Th(1)···B(2A)	156.6(2)	Th(1)···B(1)···Th(1D)	166.4(3)

[a] Symmetry transformations used to generate equivalent atoms: A = y, x, $-z$; B = $y - ½$, $-x + ½$, $z + ¼$; C = $-x + ½$, $y - ½$, $-z - ¼$; D = $-y + ½$, $x + ½$, $z - ¼$.

Table 2. Selected optimized geometry parameters for $[Th(BH_4)_6]^{2-}$ at the PBE and B3LYP levels. Experimental values are italicized.[a]

Symmetry, Environment	Level	Distances (Å)			Angles (°)				
		Th···B_t	Th···B_{b1}	Th···B_{b2}	B_t···Th···B_t	B_{b1}···Th···B_{b1}	B_{b2}···Th···B_{b2}	B_{b1}···Th···B_t	B_{b1}···Th···B_{b2}
C_2, gas	PBE/def-TZVP	2.628	2.931	2.988	113.8	153.3	78.5	86.6/78.9	102.5/98.3
C_2, COSMO	PBE/def-TZVP	2.609	2.877	2.995	118.0	159.4	74.9	89.6/79.8	102.8/93.6
C_2, gas	PBE/aVDZ	2.665	2.991	2.665	92.3	180.0	92.3	78.5/101.5	78.5/101.5
C_2, gas	PBE/aVTZ	2.665	2.992	2.665	92.2	180.0	92.2	78.6/101.4	78.6/101.4
C_2, gas	B3LYP/aVDZ	2.670	2.947	2.919	94.1	169.9	96.8	81.5/105.5	95.0/78.2
C_2, gas	B3LYP/aVTZ	2.674	2.945	2.921	93.7	169.9	93.7	81.7/105.3	94.6/78.6
C_1, gas	PBE/def-TZVP	2.663	2.992	2.663	92.1	179.9	92.1	78.5/101.4	78.5/101.4
C_1, COSMO	PBE/def-TZVP	2.648	2.967	2.648	92.9	180.0	92.9	78.1/101.8	78.2/101.8
Exptl.	—	*2.570*	*2.934*	*2.895*	*108.2*	*179.3*	*77.9*	*79.4/100.2*	*97.9/82.7*

[a] Notation: t = terminal, b_1 = bridge 1, and b_2 = bridge 2.

Table 3. Selected optimized geometry parameters for $[U(BH_4)_6]^{2-}$ at the PBE and B3LYP levels. Experimental values are italicized.[a]

Symmetry, Environment	Level	Distances (Å)			Angles (°)				
		U···B_t	U···B_{b1}	U···B_{b2}	B_t···U···B_t	B_{b1}···U···B_{b1}	B_{b2}···U···B_{b2}	B_{b1}···U···B_t	B_{b1}···U···B_{b2}
C_2, gas	PBE/def-TZVP	2.556	2.890	2.820	104.3	179.5	85.6	79.4/100.3	98.2/82.2
C_2, COSMO	PBE/def-TZVP	2.525	2.851	2.829	99.2	170.8	90.4	80.9/105.3	95.6/77.9
C_2, gas	PBE/aVDZ	2.555	2.870	2.840	96.9	170.3	93.2	81.0/105.6	105.4/77.9
C_2, gas	PBE/aVTZ	2.557	2.868	2.841	96.2	169.8	94.1	81.2/105.8	95.0/78.0
C_2, gas	B3LYP/aVDZ	2.587	2.893	2.860	96.8	170.9	93.2	80.9/105.3	95.6/78.1
C_2, gas	B3LYP/aVTZ	2.591	2.894	2.863	96.5	171.2	93.4	81.0/105.0	95.4/78.5
C_1, gas	PBE/def-TZVP	2.567	2.869	2.816	100.4	171.9	88.7	79.8/103.2	91.7/84.1
C_1, COSMO	PBE/def-TZVP	2.535	2.848	2.811	99.4	168.5	90.2	79.7/107.3	91.1/80.7
Exptl.	—	*2.521*	*2.904*	*2.820*	*110.0*	*180.0*	*80.6*	*78.7/101.1*	*96.8/83.4*

[a] Notation: t = terminal, b_1 = bridge 1, and b_2 = bridge 2.

Table 4. Selected optimized geometry parameters for $[An_3(BH_4)_{16}]^{4-}$, **3An**, and $[An_5(BH_4)_{26}]^{6-}$, **5An**, in C_2 symmetry at the PBE/def-TZVP (COSMO) level. Experimental values are italicized.[a]

	Distances (Å)			Angles (°)				
	An···B_t	An···B_{b1}	An···B_{b2}	B_t···An···B_t	B_{b1}···An···B_{b1}	B_{b2}···An···B_{b2}	B_{b1}···An···B_t	B_{b1}···An···B_{b2}
3Th	2.672	2.938	2.912	95.3	172.4	92.7	82.0/103.2	97.2/77.5
5Th	2.674	2.904	2.852	99.3	175.7	90.3	81.1/101.7	101.1/75.8
Th, *Exptl.*	*2.570*	*2.934*	*2.895*	*108.2*	*179.3*	*77.9*	*79.4/100.2*	*97.9/82.7*
3U	2.509	2.828	2.822	99.7	167.5	89.9	81.7/106.6	95.5/75.5
5U	2.502	2.826	2.809	100.9	170.7	88.6	80.5/105.5	95.3/77.9
U, *Exptl.*	*2.521*	*2.904*	*2.820*	*110.0*	*180.0*	*80.6*	*78.7/101.1*	*96.8/83.4*

[a] Notations: t = terminal, b_1 = bridge 1, and b_2 = bridge 2.

References

1. Suárez-Alcántara, K.; Garcia, J. R. T., Metal Borohydrides beyond Groups I and II: A Review. *Materials* **2021,** *14*, 2561.
2. Bannenberg, L. J.; Heere, M.; Benzidi, H.; Montero, J.; Dematteis, E. M.; Suwarno, S.; Jaron, T.; Winny, M.; Orlowski, P. A.; Wegner, W.; Starobrat, A.; Fijalkowski, K. J.; Grochala, W.; Qian, Z.; Bonnet, J. P.; Nuta, I.; Lohstroh, W.; Zlotea, C.; Mounkachi, O.; Cuevas, F.; Chatillon, C.; Latroche, M.; Fichtner, M.; Baricco, M.; Hauback, B. C.; El Kharbachi, A., Metal (Boro-)Hydrides for High Energy Density Storage and Relevant Emerging Technologies. *Int. J. Hydrogen Ener.* **2020,** *45*, 33687-33730.
3. Gu, T. T.; Gu, J.; Zhang, Y.; Ren, H., Metal Borohydride-Based System for Solid-State Hydrogen Storage. *Progr. Chem.* **2020,** *32*, 665-686.
4. Moussa, G.; Moury, R.; Demirci, U. B.; Sener, T.; Miele, P., Boron-based Hydrides for Chemical Hydrogen Storage. *Int. J. Energ. Res.* **2013,** *37*, 825-842.
5. Li, H. W.; Yan, Y. G.; Orimo, S.; Zuttel, A.; Jensen, C. M., Recent Progress in Metal Borohydrides for Hydrogen Storage. *Energies* **2011,** *4*, 185-214.
6. de Leon, C. P.; Walsh, F. C.; Pletcher, D.; Browning, D. J.; Lakeman, J. B., Direct Borohydride Fuel Cells. *J. Power Sources* **2006,** *155*, 172-181.
7. Nakamori, Y.; Li, H. W.; Matsuo, M.; Miwa, K.; Towata, S.; Orimo, S., Development of Metal Borohydrides for Hydrogen Storage. *J. Phys. Chem. Solids* **2008,** *69*, 2292-2296.
8. Schlesinger, H. I.; Brown, H. C., Uranium(IV) Borohydride. *J. Am. Chem. Soc.* **1953,** *75*, 219-221.
9. Ephritikhine, M., Synthesis, Structure, and Reactions of Hydride, Borohydride, and Aluminohydride Compounds of the f-Elements. *Chem. Rev.* **1997,** *97*, 2193-2242.

10. Jensen, J. A.; Gozum, J. E.; Pollina, D. M.; Girolami, G. S., Titanium, Zirconium, and Hafnium Tetrahydroborates as "Tailored" CVD Precursors for Metal Diboride Thin Films. *J. Am. Chem. Soc.* **1988,** *110*, 1643-1644.
11. Sung, J.; Goedde, D. M.; Girolami, G. S.; Abelson, J. R., Remote-plasma Chemical Vapor Deposition of Conformal ZrB_2 Films at Low Temperature: a Promising Diffusion Barrier for Ultralarge Scale Integrated Electronics. *J. Appl. Phys.* **2002,** *91*, 3904-3911.
12. Jayaraman, S.; Yang, Y.; Kim, D. Y.; Girolami, G. S.; Abelson, J. R., Hafnium Diboride Thin Films by Chemical Vapor Deposition from a Single Source Precursor. *J. Vac. Sci. Technol., A* **2005,** *23*, 1619-1625.
13. Jayaraman, S.; Klein, E. J.; Yang, Y.; Kim, D. Y.; Girolami, G. S.; Abelson, J. R., Chromium Diboride Thin Films by Low Temperature Chemical Vapor Deposition. *J. Vac. Sci. Technol., A* **2005,** *23*, 631-633.
14. Yang, Y.; Jayaraman, S.; Kim, D. Y.; Girolami, G. S.; Abelson, J. R., CVD Growth Kinetics of HfB_2 Thin Films from the Single-Source Precursor $Hf(BH_4)_4$. *Chem. Mater.* **2006,** *18*, 5088-5096.
15. Yang, Y.; Jayaraman, S.; Kim, D. Y.; Girolami, G. S.; Abelson, J. R., Crystalline Texture in Hafnium Diboride Thin Films Grown by Chemical Vapor Deposition. *J. Cryst. Growth* **2006,** *294*, 389-395.
16. Kumar, N.; Yang, Y.; Noh, W.; Girolami, G. S.; Abelson, J. R., Titanium Diboride Thin Films by Low-Temperature Chemical Vapor Deposition from the Single Source Precursor $Ti(BH_4)_3$(1,2-dimethoxyethane). *Chem. Mater.* **2007,** *19*, 3802-3807.
17. Yang, Y.; Jayaraman, S.; Sperling, B.; Kim, D. Y.; Girolami, G. S.; Abelson, J. R., In situ Spectroscopic Ellipsometry Analyses of Hafnium Diboride Thin Films Deposited by Single-Source Chemical Vapor Deposition. *J. Vac. Sci. Technol., A* **2007,** *25*, 200-206.

18. Kim, D. Y.; Yang, Y.; Abelson, J. R.; Girolami, G. S., Volatile Magnesium Octahydrotriborate Complexes as Potential CVD Precursors to MgB_2. Synthesis and Characterization of $Mg(B_3H_8)_2$ and its Etherates. *Inorg. Chem.* **2007,** *46*, 9060-9066.
19. Daly, S. R.; Kim, D. Y.; Yang, Y.; Abelson, J. R.; Girolami, G. S., Lanthanide N,N-Dimethylaminodiboranates: Highly Volatile Precursors for the Deposition of Lanthanide-Containing Thin Films. *J. Am. Chem. Soc.* **2010,** *132*, 2106-2107.
20. Talukdar, T. K.; Liu, S. M.; Zhang, Z. J.; Harwath, F.; Girolami, G. S.; Abelson, J. R., Conformal MgO Film Grown at High Rate at Low Temperature by Forward-Directed Chemical Vapor Deposition. *J. Vac. Sci. Technol. A* **2018,** *36*, 051504.
21. Bouix, J.; Vincent, H.; Boubehira, M.; Viala, J. C., Titanium Diboride-coated Boron Fiber for Aluminum Matrix Composites. *J. Less-Common Met.* **1986,** *117*, 83-89.
22. Caputo, A. J.; Lackey, W. J.; Wright, I. G.; Angelini, P., Chemical Vapor Deposition of Erosion-resistant Titanium Diboride (TiB_2) Coatings. *J. Electrochem. Soc.* **1985,** *132*, 2274-2280.
23. Pierson, H. O.; Randich, E., Titanium Diboride Coatings and their Interaction with the Substrates. *Thin Solid Films* **1978,** *54*, 119-128.
24. Pierson, H. O.; Randich, E.; Mattox, D. M., The Chemical Vapor Deposition of Titanium Diboride on Graphite. *J. Less-Common Met.* **1979,** *67*, 381-388.
25. Ye, W.; Martin, P. A. P.; Kumar, N.; Daly, S. R.; Rockett, A. A.; Abelson, J. R.; Girolami, G. S.; Lyding, J. W., Direct Writing of Sub-5 nm Hafnium Diboride Metallic Nanostructures. *ACS Nano* **2010,** *4*, 6818-6824.
26. Schmucker, S. W.; Kumar, N.; Abelson, J. R.; Daly, S. R.; Girolami, G. S.; Bischof, M. R.; Jaeger, D. L.; Reidy, R. F.; Gorman, B. P.; Alexander, J.; Ballard, J. B.; Randall, J. N.; Lyding, J. W., Field-directed Sputter Sharpening for Tailored Probe Materials and Atomic-scale Lithography. *Nat. Commun.* **2012,** *3*, 935.

27. Bernstein, E. R.; Keiderling, T. A.; Lippard, S. J.; Mayerle, J. J., Structure of Uranium Borohydride by Single-crystal X-ray Diffraction. *J. Am. Chem. Soc.* **1972,** *94*, 2552-2553.
28. Bernstein, E. R.; Hamilton, W. C.; Keiderling, T. A.; La Placa, S. J.; Lippard, S. J.; Mayerle, J. J., 14-Coordinate Uranium(IV). Structure of Uranium Borohydride by Single-crystal Neutron Diffraction. *Inorg. Chem.* **1972,** *11*, 3009-3016.
29. Charpin, P.; Marquet-Ellis, H.; Folcher, G., Uranium Borohydride: A New Crystalline Form. *J. Inorg. Nucl. Chem.* **1979,** *41*, 1143-1144.
30. Charpin, P.; Nierlich, M.; Vigner, D.; Lance, M.; Baudry, D., Structure of the Second Crystalline Form of $U(BH_4)_4$. *Acta Crystallogr.* **1987,** *C43*, 1465-1467.
31. Hoekstra, H. R.; Katz, J. J., The Preparation and Properties of the Group IV-B Metal Borohydrides. *J. Am. Chem. Soc.* **1949,** *71*, 2488-2492.
32. Banks, R. H. Preparation and Spectroscopic Properties of Three New Actinide(IV) Borohydrides. PhD Thesis, University of California, Berkeley, Berkeley, Ca, 1979.
33. Volkov, V. V.; Myakishev, K. G.; Grankina, Z. A., Infrared Spectra and Nature of Molecules of the Metal Borohydride-type $M(BH_4)_4$. *Russ. J. Inorg. Chem.* **1970,** *15*, 1490-1491.
34. Marks, T. J.; Kolb, J. R., Covalent Transition Metal, Lanthanide, and Actinide Tetrahydroborate Complexes. *Chem. Rev.* **1977,** *77*, 263-293.
35. Marks, T. J.; Shimp, L. A.; Kolb, J. R.; Kennelly, W. J., Structure and Dynamics in Metal Tetrahydroborates. 2. Vibrational Spectra and Structures of Some Transition-Metal and Actinide Tetrahydroborates. *Inorg. Chem.* **1972,** *11*, 2540-2546.
36. Goffart, J.; Michel, G.; Gilbert, B. P.; Duyckaerts, G., On the Indenyl Compounds of Actinide Elements. Part IV: Preparation and Properties of the Trisindenyl Thorium Tetrahydroborate. *Inorg. Nucl. Chem. Lett.* **1978,** *14*, 393-403.

37. Banks, R. H.; Edelstein, N. M.; Rietz, R. R.; Templeton, D. H.; Zalkin, A., Preparation and Properties of the Actinide Borohydrides: $Pa(BH_4)_4$, $Np(BH_4)_4$, and $Pu(BH_4)_4$. *J. Am. Chem. Soc.* **1978,** *100*, 1957-1958.

38. Banks, R. H.; Edelstein, N. M.; Spencer, B.; Templeton, D. H.; Zalkin, A., Volatility and Molecular-Structure of Neptunium(IV) Borohydride. *J Am Chem Soc* **1980,** *102*, 620-623.

39. Banks, R. H.; Edelstein, N., Synthesis and Characterization of Protactinium(IV), Neptunium(IV), and Plutonium(IV) Borohydrides In *Lanthanide and Actinide Chemistry and Spectroscopy*, Edelstein, N., Ed.; American Chemical Society: Washington, D.C., 1980; ACS Symp. Ser., Vol. 131, pp 331-348.

40. Ehemann, M.; Nöth, H., Metal Boranates and Boranatometallates. IV. Boranato Complexes $[M(BH_4)_{4+n}]^{n-}$ of Zirconium, Hafnium, and Thorium. *Z. Anorg. Allg. Chem.* **1971,** *386*, 87-101.

41. Zachariasen, W. H., Crystal Chemical Studies of the 5*f*-Series of Elements. XIX. The Crystal Structure of the Higher Thorium Hydride, Th_4H_{15}. *Acta Crystallogr.* **1953,** *6*, 393-395.

42. Turner, H. W.; Andersen, R. A.; Zalkin, A.; Templeton, D. H., Chloro-, Methyl-, and (Tetrahydroborato)tris((hexamethyldisilyl)amido)thorium(IV) and -uranium(IV). Crystal Structure of (Tetrahydroborato)tris((hexamethyldisilyl)amido)thorium(IV). *Inorg. Chem.* **1979,** *18*, 1221-1224.

43. Shinomoto, R.; Brennan, J. G.; Edelstein, N. M.; Zalkin, A., Bridging of Thorium by Hydrogen Atoms of Methyltrihydroborate Groups. Crystal Structures of Bis[tetrakis(methyltrihydroborato)thorium(IV)] Etherate and Bis[tetrakis(methyltrihydroborato)thorium(IV) tetrahydrofuranate]. *Inorg. Chem.* **1985,** *24*, 2896-2900.

44. Shinomoto, R.; Gamp, E.; Edelstein, N. M.; Templeton, D. H.; Zalkin, A., Syntheses and Crystal Structures of the Tetrakis(methyltrihydroborato) Compounds of Zirconium(IV), Thorium(IV), Uranium(IV), and Neptunium(IV). *Inorg. Chem.* **1983,** *22*, 2351-2355.
45. Trnka, T. M.; Bonanno, J. B.; Bridgewater, B. M.; Parkin, G., Bis(permethylindenyl) Complexes of Thorium: Synthesis, Structure, and Reactivity. *Organometallics* **2001,** *20*, 3255-3264.
46. McKinven, J.; Nichol, G. S.; Arnold, P. L., Arene-ligated Heteroleptic Terphenolate Complexes of Thorium. *Dalton Trans.* **2014,** *43*, 17416-17421.
47. Erickson, K. A.; Scott, B. L.; Kiplinger, J. L., $Ca(BH_4)_2$ as a Simple Tool for the Preparation of Thorium and Uranium Metallocene Borohydride Complexes: First Synthesis and Crystal Structure of $(C_5Me_5)_2Th(\eta^3\text{-}H_3BH)_2$. *Inorg. Chem. Commun.* **2017,** *77*, 44-46.
48. Dunbar, A. C.; Gozum, J. E.; Girolami, G. S., Synthesis and Characterization of Phosphine Adducts of Thorium Borohydride, $Th(BH_4)_4$: Crystal Structures of $Th(BH_4)_4(PEt_3)_2$ and $Th(BH_4)_4(Me_2PCH_2CH_2PMe_2)_2$. *J. Organomet. Chem.* **2010,** *695*, 2804-2808.
49. Daly, S. R.; Piccoli, P. M. B.; Schultz, A. J.; Todorova, T. K.; Gagliardi, L.; Girolami, G. S., Synthesis and Properties of a Fifteen-Coordinate Complex: The Thorium Aminodiboranate $[Th(H_3BNMe_2BH_3)_4]$. *Angew. Chem. Int. Ed.* **2010,** *49*, 3379-3381.
50. Settineri, N. S.; Arnold, J., Insertion, Protonolysis and Photolysis Reactivity of a Thorium Monoalkyl Amidinate Complex. *Chem. Sci.* **2018,** *9*, 2831-2841.
51. Slater, J. C., Atomic Radii in Crystals. *J. Chem. Phys.* **1964,** *41*, 3199-3204.
52. Krogh-Jespersen, K.; Romanelli, M. D.; Melman, J. H.; Emge, T. J.; Brennan, J. G., Covalent Bonding and the Trans Influence in Lanthanide Compounds. *Inorg. Chem.* **2010,** *49*, 552-560.

53. Lewis, A. J.; Mullane, K. C.; Nakamaru-Ogiso, E.; Carroll, P. J.; Schelter, E. J., The Inverse Trans Influence in a Family of Pentavalent Uranium Complexes. *Inorg. Chem.* **2014,** *53*, 6944-6953.

54. Lam, O. P.; Franke, S. M.; Nakai, H.; Heinemann, F. W.; Hieringer, W.; Meyer, K., Observation of the Inverse Trans Influence (ITI) in a Uranium(V) Imide Coordination Complex: An Experimental Study and Theoretical Evaluation. *Inorg. Chem.* **2012,** *51*, 6190-6199.

55. Gregson, M.; Lu, E.; Mills, D. P.; Tuna, F.; McInnes, E. J.; Hennig, C.; Scheinost, A. C.; McMaster, J.; Lewis, W.; Blake, A. J.; Kerridge, A.; Liddle, S. T., The Inverse-*trans*-influence in Tetravalent Lanthanide and Actinide *Bis*(carbene) Complexes. *Nat. Commun.* **2017,** *8*, 14137.

56. Piccoli, P. M. B.; Schultz, A. J.; Todorova, T. K.; Gagliardi, L.; Daly, S. R.; Girolami, G. S., Big Metals, Small Ligands: Characterization of the 15-Coordinate Complex Thorium Aminodiboranate [$Th(H_3BN(CH_3)_2BH_3)_4$] by Single Crystal Neutron Diffraction. *Am. Cryst. Assn. Symp. Trans.* **2010**, TR.01.3.

57. Vlaisavljevich, B.; Miró, P.; Koballa, D.; Todorova, T. K.; Daly, S. R.; Girolami, G. S.; Cramer, C. J.; Gagliardi, L., Volatilities of Actinide and Lanthanide *N,N*-Dimethylaminodiboranate Chemical Vapor Deposition Precursors: A DFT Study. *J. Phys. Chem. C* **2012,** *116*, 23194-23200.

58. Hu, S.-X.; Zhang, P.; Zou, W.; Zhang, P., New Theoretical Insights into High-coordination-number Complexes in Actinides-centered Borane. *Nanoscale* **2020,** *12*, 15054-15065.

Entry for the Table of Contents

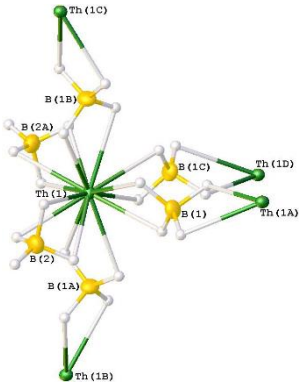

The crystal structure of $Th(BH_4)_4$ is polymeric and isomorphous with that of the tetragonal form of $U(BH_4)_4$. Each thorium center forms 14 Th–H bonds to two terminal BH_4^- ions and four κ^2,κ^2-BH_4^- ions. Fragments of the polymeric $An(BH_4)_4$ structures (An = Th, U) were also investigated by DFT. Most calculated geometries are 14-coordinate and agree with experiment, except that isolated $[Th(BH_4)_6]^{2-}$ ions are predicted to be 16-coordinate.